Published in final edited form as:

Nature. 2016 February 18; 530(7590): 293–297. doi:10.1038/nature16964.

The peptidergic control circuit for sighing

Peng Li[#1], **Wiktor A. Janczewski**[#2], **Kevin Yackle**[#1], **Kaiwen Kam**[2,Γ], **Silvia Pagliardini**[2,#], **Mark A. Krasnow**[1,**], and **Jack L. Feldman**[2,**]

[1] Department of Biochemistry and Howard Hughes Medical Institute, Stanford University School of Medicine, Stanford, CA, 94305

[2] Systems Neurobiology Laboratory, Department of Neurobiology, David Geffen School of Medicine, University of California Los Angeles, Los Angeles, CA, 90095

[#] These authors contributed equally to this work.

Abstract

Sighs are long, deep breaths expressing sadness, relief, or exhaustion. Sighs also occur spontaneously every few minutes to reinflate alveoli, and sighing increases under hypoxia, stress, and certain psychiatric conditions. Here we use molecular, genetic, and pharmacologic approaches to identify a peptidergic sigh control circuit in murine brain. Small neural subpopulations in a key breathing control center (RTN/pFRG) express bombesin-like neuropeptide genes neuromedin B (*Nmb*) or gastrin releasing peptide (*Grp*). These project to the preBötzinger Complex (preBötC), the respiratory rhythm generator, which expresses NMB and GRP receptors in overlapping subsets of ~200 neurons. Introducing either neuropeptide into preBötC, or onto preBötC slices, induced sighing, whereas elimination or inhibition of either receptor reduced basal sighing and inhibition of both abolished it. Ablating receptor-expressing neurons eliminated basal and hypoxia-induced sighing, but left breathing otherwise intact initially. We propose these overlapping peptidergic pathways comprise the core of a sigh control circuit that integrates physiological and perhaps emotional input to transform normal breaths into sighs.

Introduction

A sigh is a long deep breath often associated with sadness, yearning, exhaustion or relief. Sighs also occur spontaneously, from several per hour in humans to dozens per hour in

[**] Corresponding authors. Correspondence and requests for materials should be addressed to M.A.K. (krasnow@stanford.edu), 650-723-7191 (phone); 650-723-6783(fax)), or J.L.F. (feldman@g.ucla.edu)..

[Γ] Current address: Department of Cell Biology and Anatomy, Chicago Medical School, Rosalind Franklin University of Medicine and Science, North Chicago, IL, 60064

[#] Current address: Department of Physiology, University of Alberta, Edmonton, AB T6G 2E1 Canada

Author Contributions

W.A.J. and S.P. performed experiments showing effects on sighing of bombesin injection into the preBötC and ablation of receptor-expressing neurons with bombesin-saporin. K.Y. performed screen that discovered *Nmb* expression in the respiratory centers. P.L. performed experiments identifying and characterizing expression of *Nmb*, *Grp* and their receptors. W.A.J., P.L., K.Y. performed genetic and pharmacology experiments on *Nmb* and *Grp* pathways. K.K. performed *in vitro* slice experiments. W.A.J., K.K., P.L., S.P., and K.Y. analyzed data. J.L.F., W.A.J., K.K., M.A.K., P.L., K.Y. conceived experiments, interpreted data and wrote manuscript.

The authors declare no competing financial interests.

Supplementary Information is linked to the online version of the paper at www.nature.com/nature.

rodents[1,2]. Their recurrence during normal breathing enhances gas exchange and may preserve lung integrity by reinflating collapsed alveoli[2-4]. Sighing increases in response to emotional and physiological stresses, including hypoxia and hypercapnia, and in anxiety disorders and other psychiatric conditions where it can become debilitating[5,6].

The kernel of the breathing rhythm generator is the preBötC, a cluster of several thousand neurons in ventrolateral medulla. preBötC is required for inspiration and generates respiratory rhythms in explanted brain slices[7-10]. Each rhythmic burst activates premotoneurons and motoneurons that contract the diaphragm and other inspiratory muscles, generating a normal ("eupneic") breath[10]. Occasionally, a second preBötC burst immediately follows the first, and this "double burst" leads to the augmented inspiration of a sigh[11-13], typically about twice the volume of a normal breath[14]. Thus, the command for normal breaths and sighs both appear to emanate from preBötC.

A variety of neuromodulators and neuropeptides[15,16], including frog bombesin[15], can influence sighing in rodents. However, the endogenous sigh control pathways have not been identified. We tested the effect of injecting bombesin into preBötC[17], and we screened for genes selectively expressed in breathing control centers (K.Y. and M.A.K., in preparation). These parallel approaches led to identification of two bombesin-like neuropeptide pathways connecting the retrotrapezoid nucleus/parafacial respiratory group (RTN/pFRG), another medullary breathing control center[18,19], to preBötC. We provide genetic, pharmacologic and neural ablation evidence that these pathways are critical endogenous regulators of sighing and define the core of a dedicated sigh control circuit.

Results

Neuromedin B links two breathing control centers

To identify breathing control genes, we screened >19,000 gene expression patterns in embryonic day 14.5 mouse hindbrain[20] (K.Y. and M.A.K., in preparation). The most specific pattern was neuromedin B (*Nmb*), one of two genes encoding bombesin-like neuropeptides in mammals. *Nmb* is expressed in the medulla surrounding the lateral half of the facial nucleus, in or near RTN/pFRG in mouse (Fig. 1a,b) and rat (ED Fig. 1a,b). *Nmb* mRNA was also detected in olfactory bulb and hippocampus (ED Fig. 1c,d).

Nmb expression was further characterized using an Nmb-GFP BAC transgene, which reproduced the endogenous *Nmb* pattern (Fig. 1b, c). Nmb-GFP expressed in 206±21 (mean ±S.D., n=4) RTN/pFRG neurons per side, most of which (92%, n=53 cells scored) co-expressed *Nmb* mRNA (ED Fig. 1e-h). In CLARITY-processed brainstems, GFP-labeled cells surrounded the lateral half of the facial nucleus, with highest density ventral and dorsal (Fig. 1d,e; Supplementary Video 1). This ventral parafacial region is the RTN, an important sensory integration center for breathing[18,21,22]. Nearly all Nmb-GFP-positive cells (96%; n=202 cells from 2 animals) co-expressed canonical RTN marker PHOX2B[23] (Fig. 1f), comprising one-fourth of the ~800 PHOX2B-positive RTN neurons[24].

Nmb-expressing neurons projected to preBötC (Fig. 1g,j). Punctate NMB staining was detected along the projections (ED Fig. 2), some puncta abutting somatostatin-positive

preBötC neurons (Fig. 1h; ED Fig. 2). ~90 preBötC neurons expressed *Nmbr*, the GPCR specific for NMB (Fig. 1i, see below). Thus, *Nmb*-expressing RTN/pFRG neurons may directly modulate preBötC neurons.

NMB injection into preBötC induces sighing

To investigate function of this NMB pathway, the peptide was microinjected into preBötC of urethane-anesthetized adult rats. Before injection, and after control (saline) injections, airflow and diaphragmatic activity (DIA_{EMG}) showed the normal (eupneic) breathing pattern, with diaphragm activity bursts during inspiration (Fig. 2a, ED Fig. 3a). Every minute or two, we observed a sigh (44±10/hour, n=24; unaffected by saline injection, ED Fig. 3b), a biphasic double-sized breath coincident with a bimodal DIA_{EMG} event (Fig. 2c and ED Fig. 3a,c-f). Amplitude and timescale of the first component of a sigh was indistinguishable from eupneic breaths, like human sighs[25]. Following bilateral NMB microinjection (100nl, 3μM) into preBötC, sighing increased 6-17-fold (n=5; Fig. 2d, ED Fig. 4a-e). Effect peaked several minutes after injection and persisted 10-15 minutes afterwards.

We also tested NMB on explanted preBötC brain slices of neonatal mice, where inspiratory activity is detected as rhythmic bursts of preBötC neurons and hypoglossal (cranial nerve XII) motoneuron output (Fig. 2e). Occasionally, a burst with two peaks (“doublet”) was observed (Fig. 2e)[11], a proposed *in vitro* signature of a sigh (Methods). Addition of 10nM and 30nM NMB increased doublet frequency 1.7-fold (p=0.005; n=7) and 2-fold, respectively (p=0.003; n=7) (Fig. 2e,f). Overall frequency of bursts and doublets together was unchanged (p=0.2; n=7), implying NMB converts inspiratory bursts into sighs; indeed, in some preparations every inspiratory burst was converted to a doublet (ED Fig. 5). We conclude NMB acts directly on preBötC to increase sighing.

NMBR signaling maintains basal sighing

To determine if NMB signaling is required for sighing, we monitored breathing of awake, unrestrained $Nmbr^{-/-}$ knockout mice. Wild type controls (C57BL/6) sighed 40±11/hour, whereas $Nmbr^{-/-}$ mutants sighed 29±10/hour (n=4; p<0.001) (Fig. 2g). Sighing was also transiently reduced ~50% in anesthetized rats by NMBR inhibition following bilateral preBötC injection of the antagonist BIM23042 (100nl, 6μM) (Fig. 2h, ED Fig. 6a-d,7a). The antagonist effect was selective for sighing as it did not significantly alter respiratory rate (117±14 vs. 109±6 breaths/minute with antagonist, n=4, p=0.14) or tidal volume (2.1±0.1 vs. 2.0±0.3 ml, n=4, p=0.46), and similar selectivity was observed for the *Nmbr* mutant (respiratory rate 218±22 vs. 254±22 in $Nmbr^{-/-}$mice, n=4, p=0.06; tidal volume 0.30±0.03 vs. 0.31±0.04 ml, n=4, p=0.88). Thus NMBR signaling in preBötC maintains basal sighing.

Another bombesin-like neuropeptide pathway also modulates sighing

Nmbr mutations and inhibition reduced but did not abolish sighing, suggesting involvement of other pathways. Gastrin-releasing peptide (*Grp*), the only other bombesin-like neuropeptide gene in mammals[26], was expressed in several dozen cells in the dorsal RTN/pFRG in mouse (Fig. 3a) and rat (ED Fig. 8e) plus scattered cells in nucleus tractus solitarius (NTS) and parabrachial nucleus (PBN), two other breathing circuit nuclei[10,27] (ED

Fig. 8a-d). GRP-positive projections were traced from RTN/pFRG to preBötC, some GRP puncta abutting SST-positive preBötC neurons (ED Fig. 8f-i). GRP signals through GRPR, the receptor most similar to NMBR. *Grpr* mRNA was detected in ~160 mouse preBötC neurons (Fig. 3b and see below), suggesting GRP may also directly modulate preBötC function.

To determine if GRP regulates sighing, the neuropeptide (100nl, 3μM) was injected bilaterally into preBötC of anesthetized rats. Sighing increased 8-16-fold (n=5; Fig. 3c, ED Fig. 4f-j). GRP (3nM) application to mouse preBötC brain slices also increased sighing, showing 1.7-fold more doublets (p=0.003; n=9; Fig. 3d). Thus, GRP can induce sighing through direct modulation of preBötC neurons, like NMB.

To determine if GRPR signaling is required for sighing, we monitored breathing in $Grpr^{-/-}$ knockout mice. Their basal sigh rate (22±9 /hour, n=4) was half that of control wild type mice (Fig. 3e), whereas eupneic breathing appeared normal (respiratory rate 218±22 vs. 210±16 in $Grpr^{-/-}$, n=4, p=0.57; tidal volume 0.30±0.03 vs. 0.28±0.01 ml, n=4, p=0.23). GRPR inhibition by bilateral preBötC injection of antagonist RC3095 (100nl, 6μM) in anesthetized rats also transiently decreased sighing by ~50% (n=4), followed by rapid rebound and overshoot (Fig. 3f, ED Fig. 6e-h). There was no significant change in other respiratory parameters (respiratory rate 117±12 vs. 111±11 with antagonist, n=4, p=0.34; tidal volume 2.0±0.2 vs. 1.9±0.1 ml, n=4, p=0.11). Thus, GRPR signaling in preBötC also maintains basal sighing.

Expression patterns, loss-of-function phenotypes and localized pharmacological manipulations of NMBR and GRPR signaling in preBötC suggest that NMB-NMBR and GRP-GRPR pathways can independently modulate sighing.

NMBR and GRPR are the critical pathways in sighing

To explore the relationship between NMB and GRP pathways, we compared expression patterns of the neuropeptides and receptors within mouse RTN/pFRG and preBötC. *Nmb* and *Grp* were detected in non-overlapping neuronal subpopulations, with *Nmb* neurons distributed throughout RTN/pFRG and *Grp* neurons restricted to the dorsal domain (Fig. 4a-d). In contrast, receptor expression patterns in preBötC overlapped (Fig. 4e-h), with 40±16 neurons expressing *Nmbr*, 113±45 expressing *Grpr*, and 49±9 expressing both (n=3).

To explore functional interactions, we injected both neuropeptides into preBötC of anesthetized rats. Sigh rate increased 12-24-fold, similar or slightly beyond that of either neuropeptide alone (Fig. 4i, ED Fig. 4k-o). When NMBR and GRPR pathways were simultaneously inhibited by bilateral injection of both antagonists, BIM23042 (100nl, 6μM) and RC3095 (100nl, 6μM), sighing was severely reduced or eliminated (n=6; Fig. 4j, ED Fig. 6i-n). Thus, NMBR and GRPR pathways can independently modulate sighing, and together are required for basal sighing *in vivo*.

Effect of NMBR and GRPR neuron ablation

To determine if preBötC NMBR- and GRPR-expressing neurons function specifically in sigh control, we ablated them using bombesin (BBN), which binds both receptors[26],

conjugated to saporin (BBN-SAP), a ribosomal toxin that induces neuron death when internalized[8]. Three days after bilateral BBN-SAP injection (200nl, 6.15ng/side) into preBötC of rats, sighing was reduced ~80%, from 24±1/hour before injection to 5±2/hour three days after injection ($p=5\times10^{-6}$; n=7) (Fig. 5a). The effect was selective as other aspects of breathing and behavior appeared normal. Five days after injection, sighing was almost completely (~95%) abolished, decreasing to 0.6±0.3/hour ($p=10^{-8}$; n=6; Fig. 5a). Other aspects of breathing and behavior again appeared generally intact (ED Fig. 9a, b). However, after five days we noted occasional brief episodes of apneas or disordered breathing, possibly a consequence of the loss of sighing (see Discussion). Ablation prevented sigh induction by exogenous BBN infusion into the cisterna magna, confirming preBötC *Nmbr*- and *Grpr*-expressing neurons were eliminated (ED Fig. 9c). However, BBN infusion still triggered intense scratching and licking, demonstrating that the *Grpr* and *Nmbr* neurons outside the preBötC required for these behaviors[28] remained intact. We conclude that preBötC *Nmbr* and *Grpr*-expressing neurons have a critical and selective function in basal sighing.

NMBR and GRPR neurons are also critical for hypoxia-induced sighing

To determine if the *Nmbr* and *Grpr*-expressing neurons are also important for physiologically-induced sighs, we examined BBN-SAP rats exposed to hypoxia (8% O_2). In control rats injected with unconjugated SAP, sighing increased from 24±5 to 140±8/hour under hypoxia (n=3, p=0.01). In contrast, five days after BBN-SAP injection, sigh rate under hypoxia was 5.1±3.2/hour (n=6, p=0.2; Fig. 5b); three of these rats did not sigh in room air (21% O_2) and no sighs were triggered by hypoxia. In BBN-SAP rats, hypoxia increased respiratory rate from 150±1 to 230±3 breaths/min, demonstrating ventilatory response to hypoxia was intact. Thus, *Nmbr* and *Grpr*-expressing neurons are also critical for hypoxia-induced sighing, but not other respiratory responses to hypoxia.

Discussion

Our results show sighing is controlled by two largely parallel bombesin-like neuropeptide pathways, NMB and GRP, which mediate signaling between key medullary breathing control centers. ~200 *Nmb*-expressing and ~30 *Grp*-expressing neurons in neighboring domains of RTN/pFRG, a region implicated in integrating respiratory sensory cues and generation of active expiration[22,27,29], project to preBötC, the respiratory rhythm generator. 7% (~200) of preBötC neurons express *Nmbr* (~40 neurons), *Grpr* (~110), or both receptors (~50), activation of which increased sighing 6 to 24-fold, whereas sighing was effectively abolished by inhibition or deletion of the receptors, or ablation of the receptor-expressing neurons.

We propose the above neurons, perhaps with *Grp*-expressing NTS and PBN neurons, comprise the core of a peptidergic sigh control circuit, with the neuropeptide-expressing neurons integrating inputs from sites monitoring physiological and perhaps emotional state (Fig. 5c). Excitation of these neurons and secretion of either neuropeptide activates the cognate receptor-expressing preBötC neurons, which initiate sighs by altering activity of other preBötC neurons to convert normal breaths to sighs. This might occur by a burst of

NMB and/or GRP secretion triggering a second inspiratory signal in the preBötC during or immediately after the first, resulting in a single, double-size breath. Alternatively, NMB and GRP secretion might be more gradually modulated, causing concentration-dependent bursts in activity of receptor-expressing neurons or shift in preBötC properties toward states favoring more frequent doublet bursts.

A priority now is to elucidate the full circuit and properties of the constituent neurons, including its integration with other peptides and neurotransmitters that influence sighing[15,16] and with normal breathing and other behaviors. One curious aspect of the circuit already apparent is the central role of two partially-overlapping and closely-related neuropeptide pathways. Do NMB- and GRP-expressing neurons receive different inputs and have distinct sensing functions, and do the three sets of receptor-expressing neurons (NMBR, GRPR, NMBR+GRPR) converge on the same preBötC neurons to effect a sigh, or signal to different preBötC neurons producing distinct types of sighs?

A striking aspect of our results is the selectivity of the circuit for sighing. Inhibition of the pathways, and even ablation of receptor-expressing neurons, had little effect on other aspects of breathing, at least in the short term. This can now be exploited to test the classical idea of sighing's physiological function -- reexpansion of alveoli that collapse during breathing and maintenance of lung integrity[2-4], and investigate psychological benefits. Identification of the key neuropeptide pathways suggests pharmacologic approaches for controlling excessive sighing and inducing sighs in patients that cannot breathe deeply on their own. Dozens of molecularly distinct preBötC neuronal types have been identified recently (K.Y. and M.A.K., unpublished); perhaps they serve similarly specific roles in other respiratory-related behaviors like yawning, sniffing, crying, and laughing.

Methods

Animals

All procedures were carried out in accordance with animal care standards in National Institutes of Health (NIH) guidelines, and approved by the University of California, Los Angeles Animal Research Committee, or Stanford Institutional Animal Care and Use Committee. All mouse strains used were in the C57BL/6 genetic background. Nmb-GFP BAC transgenic mice (Tg(Nmb-EGFP)IT50Gsat/Mmucd), carrying EGFP coding sequence inserted upstream of the Nmb start codon in the BAC, were from the Mutant Mouse Regional Resource Centers (catalog number 030425-UCD, https://www.mmrrc.org). *Nmbr*$^{-/-}$ and *Grpr*$^{-/-}$ null mutant mice, in which exon 2 of the endogenous gene was replaced by a neomycin-resistance cassette using homologous recombination, have been described[30,31]. Male Sprague Dawley rats were from Charles River.

In situ hybridization, immunostaining and reporter expression

For *in situ* hybridization, mouse brains were harvested and fixed overnight in 4% paraformaldehyde in phosphate buffered saline (PBS), cryopreserved in 30% sucrose and embedded in optical cutting temperature compound (OCT). Transverse sections were cut at 16 - 20 microns and stored at −80°C until use. Sections were post-fixed in 4%

paraformaldehyde before treatment with hydrochloric acid, proteinase K, and then triethanolamine/acetic anhydride. Hybridization was carried out with *in vitro* transcribed and digoxygenin-labeled riboprobes at 58°C overnight. Signal was detected using Alkaline Phosphatase-coupled anti-Digoxigenin (DIG) primary antibody (Roche) and nitro blue tetrazolium chloride and bromochloroindolyl phosphate (NBT/BCIP) Reagent Kit (Roche) or using Horse Radish Peroxidase-coupled anti-DIG primary antibody (Roche) and Tyramide Signal Amplification plus Fluorescent Substrate Kit (PerkinElmer).

For double fluorescent *in situ* hybridization, tissue was harvested, embedded in OCT and then sectioned. Sections were fixed in 4% paraformaldehyde, dehydrated and treated with pretreatment reagent (Advanced Cell Diagnostics). Double fluorescent in situ assay was then performed using proprietary RNAscope technology (Advanced Cell Diagnostics) with cyanine 3-labeled *Nmbr* probes and fluorescein isothiocyanate-labeled *Grpr* probes.

For Nmb-GFP reporter expression analysis, the brains of Nmb-GFP postnatal day 0 mice were harvested and fixed overnight in 4% paraformaldehyde and then cryopreserved at 4°C in 30% sucrose overnight. Tissue was embedded in OCT and sectioned at 10 - 40 microns. Tissue sections were rinsed with PBT (PBS + 0.1% Tween), blocked with 3% bovine serum (BSA) in PBT for 1hr, and incubated with primary antibody overnight at 4°C. Sections were rinsed in PBT and incubated for 1 hour at room temperature with species-specific secondary antibodies. Primary antibodies were: chicken anti-GFP (Abcam 13970; used at 1:1000 dilution), goat anti-PHOX2B (Santa Cruz, sc-13224; 1:200 dilution), rabbit anti-NMB (Sigma-Aldrich, SAB1301059; 1:100 dilution), rabbit anti-GRP (Immunostar 20073; 1:4000 dilution), and rat anti-SST (Millipore, MAB354; 1:50 dilution). Secondary antibodies included donkey anti-chicken (Jackson Immuno Research; 1:400 dilution), donkey anti-rat (Jackson Immuno Research; 1:400 dilution), donkey anti-rabbit (Jackson Immuno Research; 1:400 dilution) and donkey anti-goat (Invitrogen; 1:500 dilution).

For Nmb-GFP expression analysis in samples prepared by CLARITY[32], Nmb-GFP mice were perfused with PBS and formaldehyde-acrylamide hydrogel, and brain tissue was harvested and incubated in hydrogel monomer solution at 4 °C for 3 days. Tissue was then embedded in polymerized hydrogel by raising the temperature to 37°C for 3 h. Blocks of 1 mm thickness were cut and washed in 4% sodium dodecyl sulfate (SDS) in sodium borate buffer at 37°C for 2 - 3 weeks. Samples were washed with PBST for 2 days and incubated in FocusClear (CelExplorer), and GFP fluorescence was imaged on a Zeiss LSM780 confocal microscope.

Sigh monitoring and analysis

For awake animals, individual animals were placed in a whole body plethysmography chamber (Buxco) at room temperature (22°C) in 21% O_2 (for normoxia) or 8% O_2 (for hypoxic challenge) balanced with N_2. Sighs were identified in plethysmography traces by the characteristic biphasic ramp, the augmented flow in the second phase of the inspiratory effort and the prolongation of expiratory time following the event. Sighs were also confirmed by visual monitoring of breathing behavior. Given the high amplitude and distinctive waveform of sighs relative to standard eupneic breaths, sighs were unambiguously identified by both visual and computer-assisted scoring; no difference was

detected in direct comparisons between methods or observers so visual scoring was used. Female 8 week old mice (*Nmbr*$^{-/-}$, *Grpr*$^{-/-}$, or C57BL/6 as wild type control) were allowed to acclimate for 10 minutes in the chamber, and then the first fifteen recorded sighs were used to calculate the sigh rate. Similar sigh rates were observed for each animal when assayed on different days. Rats were allowed to acclimate in the chamber for ~1 hr, and then baseline sigh rate and respiratory frequency were calculated for the next 2 hrs. For hypoxic (8% O_2) challenge, analysis was continued for 30 minutes under the hypoxic condition.

For anesthetized rats, the trachea was cannulated and connected to a pneumotachograph (GM Instruments) to record airflow. A flow calibration was performed after every experiment along with a calculation of tidal volume (V_T) by digital integration. To monitor diaphragm activity, wire electrodes (Cooner Wire) were implanted into the diaphragm and electromyogram (EMG) signal sampled at 2 kHz (Powerlab 16SP; AD Instruments). Signal was rectified and digitally integrated (time constant of 0.1) to obtain a moving average using LabChart Pro 8 (AD Instruments) and Igor Pro 6 (Data Matrix) software. Sighs were identified in the airflow measurements as above and validated by double peaks in the EMG recordings.

preBötC injection of NMB and GRP agonists and antagonists

Male Sprague Dawley rats (n=24) weighing 320–470 g were anesthetized with urethane (1.5 g/kg), isoflurane (0.3-0.7 vol%), and ketamine (20 mg/kg/hour) and injected i.p. with atropine (0.3 mg/kg), then placed in a supine position in a stereotaxic instrument (David Kopf Instruments). A tracheostomy tube was placed in the trachea through the larynx, and the basal aspect of the occipital bone was removed to expose the ventral medulla. Injections were placed 750 μm caudal from the most rostral root of the hypoglossal nerve (RRXII), 2 mm lateral to the midline, and 700 μm dorsal to the ventral medullary surface. Small corrections were made to avoid puncturing blood vessels on the medulla. Microinjection was done using a series of pressure pulses (Picospritzer; Parker-Hannifin) applied to the open end of micropipettes, with air pressure set so that each pulse ejected ~5 nl and a total volume of 0.1 μl was injected on each side. The concentration of injected neuropeptides and antagonists were: NMB, 3 μM; GRP, 3 μM; NMB and GRP, 3 μM each; BIM23042[33], 6 μM; RC3095[34], 6 μM; BIM23042 and RC3095, 6 μM each. To verify the accuracy of the injections, fluorescent polystyrene beads (0.2 μm FluoSpheres (Invitrogen; catalog #F8811, #F8763 or #F8807); 2–5% vol) were added to the injected solutions, and following injection and physiological measurements the location of the fluorescent beads was visualized in freshly cut wet tissue double-DAB stained for reelin and choline acetyltransferase (ChAT) to identify the preBötC.

Ablation of NMBR and GRPR-expressing preBötC neurons

Bilateral preBötC injections of saporin conjugated with either bombesin (BBN-SAP; Advanced Targeting System; 200 nl, 6.2 ng) or a non-targeted peptide (blank SAP; Advanced Targeting System; 200 nl, 6.2 ng) were performed in 300-350 g rats under anesthesia (ketamine (90 mg/kg), and xylazine (10 mg/kg), administered i.p) using standard aseptic procedures. Rats were positioned on a stereotaxic frame with bregma 5 mm below lambda. The occipital bone was exposed and a small window was opened to perform BBN-

SAP injections with a 40 μm diameter tip glass pipette inserted into the preBötC. Coordinates were (in mm): 0.9 rostral, 2.0 lateral, and 2.8 ventral to the obex. The electrode was left in place for 5 min after injection to minimize backflow of solution up the electrode track. After injection, a fine polyethylene cannula was implanted and cemented to the occipital bone to deliver BBN into the fourth ventricle. Neck muscles and skin were sutured back at the end of the surgery and rats were allowed to recover with pain medication, food and water ad libitum. Blank-SAP and BBN-SAP treated rats were tested for hypoxia (8% O2 balanced with nitrogen, 30 minute challenge) five days after surgery. Blank-SAP and BBN-SAP treated rats were also tested for response to BBN infusion in the intracerebellomedullary space six days after surgery. The cannula implanted in the fourth ventricle was connected to a fine polyethylene tubing under isoflurane anesthesia, and after recovery and placement of rats in a plethysmographic chamber 10 μg of BBN diluted in 20 μl sterile saline was delivered followed by a 20 μl saline washout. Sigh rate and respiratory rate were calculated for 30 minutes following infusion and compared to pre-infusion values.

In vitro slice preparation, recording, and analysis

Rhythmic 550-μm-thick transverse medullary slices containing the preBötC and XII nerve from neonatal C57BL/6 mice (P0-5) were prepared as described previously (Kam et al., 2013). The medullary slice was cut in artificial cerebrospinal fluid (ACSF) containing (in mM): 124 NaCl, 3 KCl, 1.5 $CaCl_2$, 1 $MgSO_4$, 25 $NaHCO_3$, 0.5 NaH_2PO_4, and 30 D-glucose, equilibrated with 95% O_2 and 5% CO_2 (4°C, pH=7.4). For recording, extracellular K^+ was raised to 9 mM to replace excitatory afferent drive lost in the cutting process. Slices were perfused at 27°C and 4 ml/min and allowed to equilibrate for 30 minutes. Respiratory activity reflecting suprathreshold action potential (AP) firing from populations of neurons was recorded as XII bursts from either XII nerve roots and as population activity directly from the preBötC using suction electrodes and a MultiClamp 700A or 700B (Molecular Devices, Sunnyvale, CA, USA), filtered at 2–4 kHz and digitized at 10 kHz. Digitized data were analyzed off-line using custom procedures written for IgorPro (Wavemetrics, Portland, OR, USA). Activity was full-wave rectified and digitally integrated with a Paynter filter with a time constant of 20 ms with either custom built electronics or using custom procedures in MATLAB (Mathworks, Natick, MA, USA).

Burst detection and analysis of respiratory-related activity recorded in full-wave rectified XII output or preBötC population recordings were performed using custom software written in IgorPro. Burst parameters were normalized to the mode of the data in the baseline condition. Although there are several proposed definitions of sighs in slice preparations[12,13], here we used “doublets” (double-peaked bursts) as the *in vitro* signature of sighs because, in our preparations, doublets detected both in preBötC neural population activity measurements and cranial nerve XII output recordings shared the increased inspiratory and expiratory duration of sighs[11]. Furthermore, as demonstrated here, doublet rate increased following application of NMB or GRP to preBötC slice preparations (Figs. 2, 3, ED Fig. 5), as did sigh rate *in vivo* following preBötC injection of the same neuropeptides (Figs. 2, 3). The frequency and waveform of doublets in slice preparations does not closely match those of sighs in intact animals, presumably due to the absence *in vitro* of important inputs modulating burst shape; indeed, the doublets more closely resemble sighs in vagotomized

animals, where they appear as equal amplitude double-peaked breaths[11, 17]. We scored a burst as a doublet if the burst displayed a second peak that reached 20% or more of the amplitude of the first burst, and this second peak occurred after more than twice the time from start to peak or if the burst had a duration longer than eight times the time from start to peak. All doublets were verified by visual inspection to exclude multipeaked bursts and two bursts that were too far apart. Measured doublet intervals were converted to a calculated per hour doublet rate.

Statistics

Data are represented as mean±standard deviation (SD). Statistical significance was uniformly set at a minimum of $p<0.05$. For comparisons of two groups, the assumption for normal distribution was determined by the Shapiro-Wilk test with the critical W value set at 5% significance level. The t-tests were conducted, with the exception in Figure 3e, in which a Mann-Whitney U test was used. For statistical comparisons of more than two groups, an ANOVA was first performed. In most cases, a two-way repeated measures ANOVA was used for comparisons of various parameters in different conditions and for making comparisons across different events. If the null hypothesis (equal means) was rejected, post-hoc paired t-tests were then used for pairwise comparisons of interest. Individual p-values are reported, but Holm-Bonferroni analysis for multiple comparisons was conducted to correct for interactions between the multiple groups. Histograms were normalized by the total sample size to generate plots of the relative frequency of each value where the y-value of each bin represents the fraction of the total number of samples for that experiment. Randomization and blinding were not used. No statistical method was used to predetermine sample size.

Extended Data

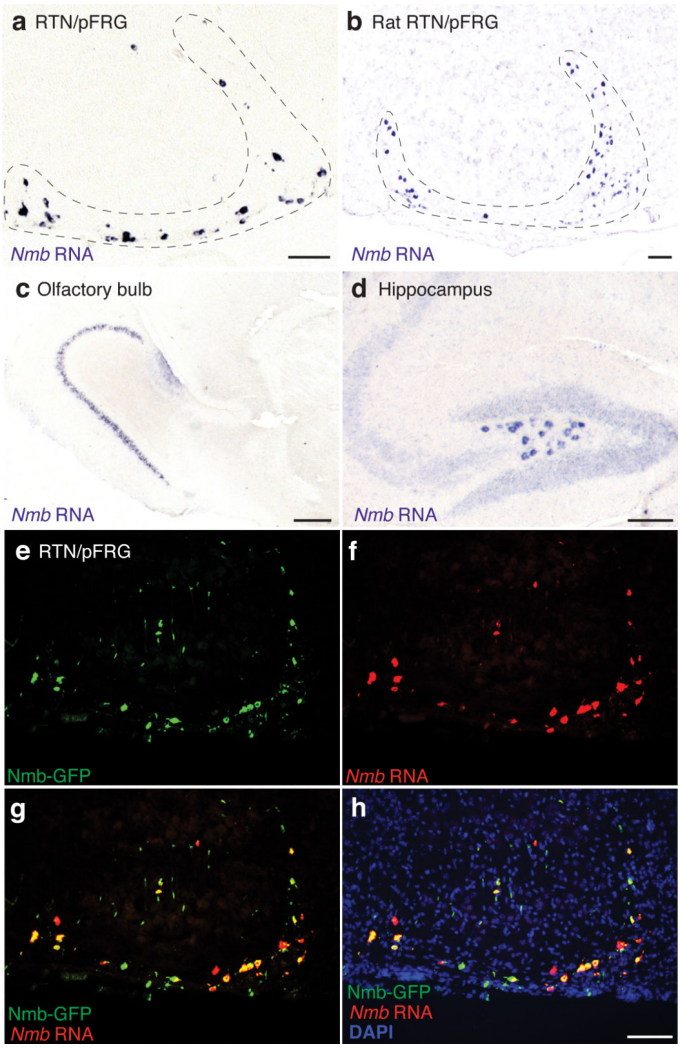

Extended Data Figure 1. Expression of neuromedin b (*Nmb*) in rodent brain

a, b, Sagittal sections of P7 mouse (a) and P7 rat (b) brain showing RTN/pFRG region probed for *Nmb* mRNA expression (purple) by *in situ* hybridization as in Figure 1. Bars, 100 μm. **c, d**, *Nmb* expression as in a showing regions outside ventrolateral medulla. *Nmb* is expressed in mouse olfactory bulb (c) and hippocampus (d). Bars, 200 μm (c) and 100 μm (d). **e-h,** Section through RTN/pFRG brain region of P0 transgenic Nmb-GFP mouse immunostained for GFP (green) and probed for *Nmb* mRNA (red) by *in situ* hybridization. Blue, DAPI nuclear stain. Nmb-GFP and *Nmb* mRNA are largely co-expressed in same cells. Bar, 100 μm.

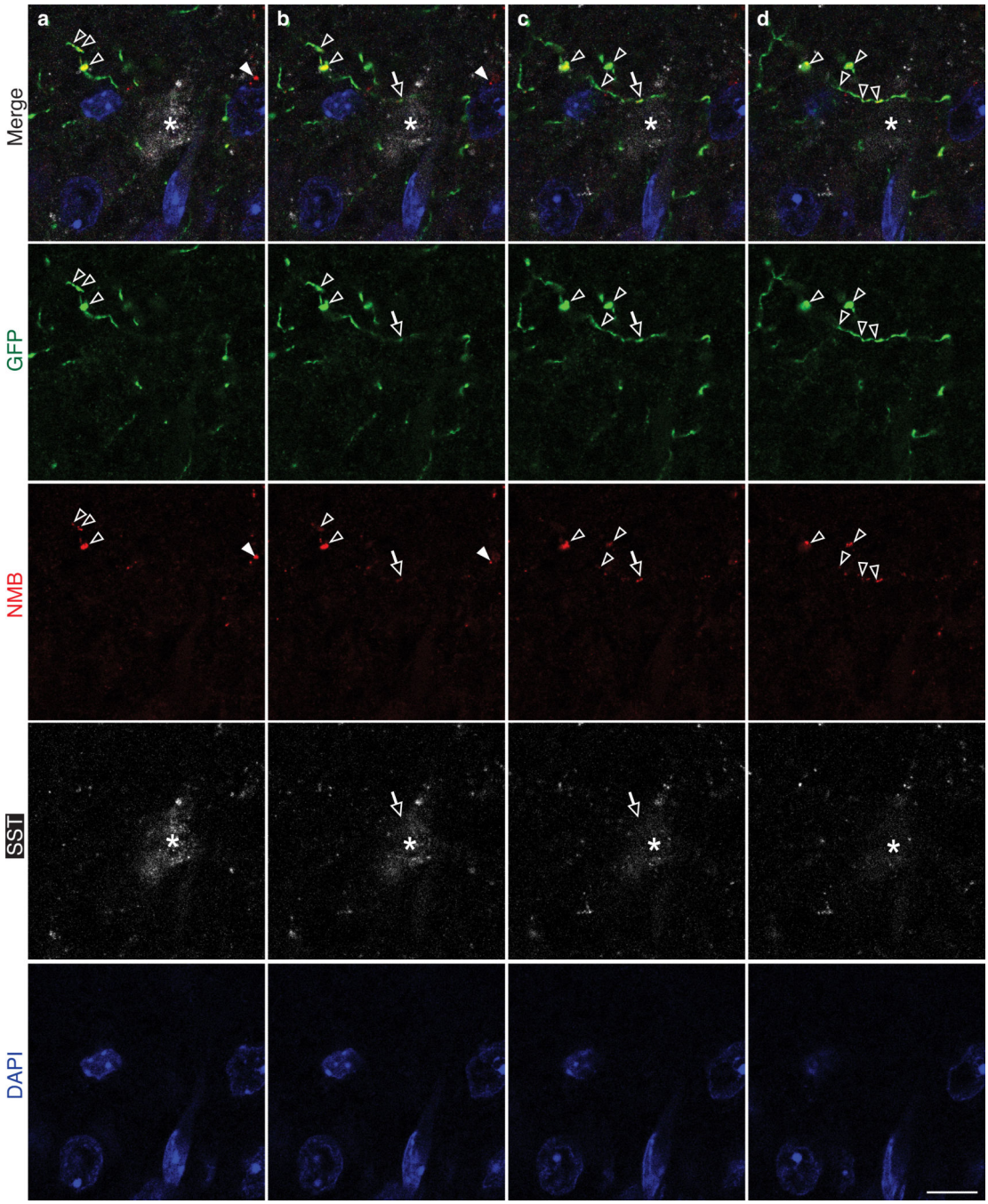

Extended Data Figure 2. Serial confocal preBötC sections showing Nmb-GFP projections contain puncta of NMB

a-d, Serial confocal optical sections (0.6 μm apart) through preBötC brain region of Nmb-GFP mouse immunostained for GFP (green), NMB (red), preBötC marker SST (white), and DAPI (blue) as in Figure 2h. Note the GFP-positive projection with a puncta of NMB (yellow, open arrows in b,c) directly abutting an SST positive neuron (asterisk). Most NMB puncta (open arrowheads) were detected within GFP-positive projections as expected, and only a small fraction of NMB puncta (closed arrowhead) were detected outside them; NMB

outside Nmb-GFP projections could be secreted protein or the rare *Nmb*-expressing cells that do not co-express the *Nmb-GFP* transgene (see Extended Data Figure 1e-h). Bar, 20 μm.

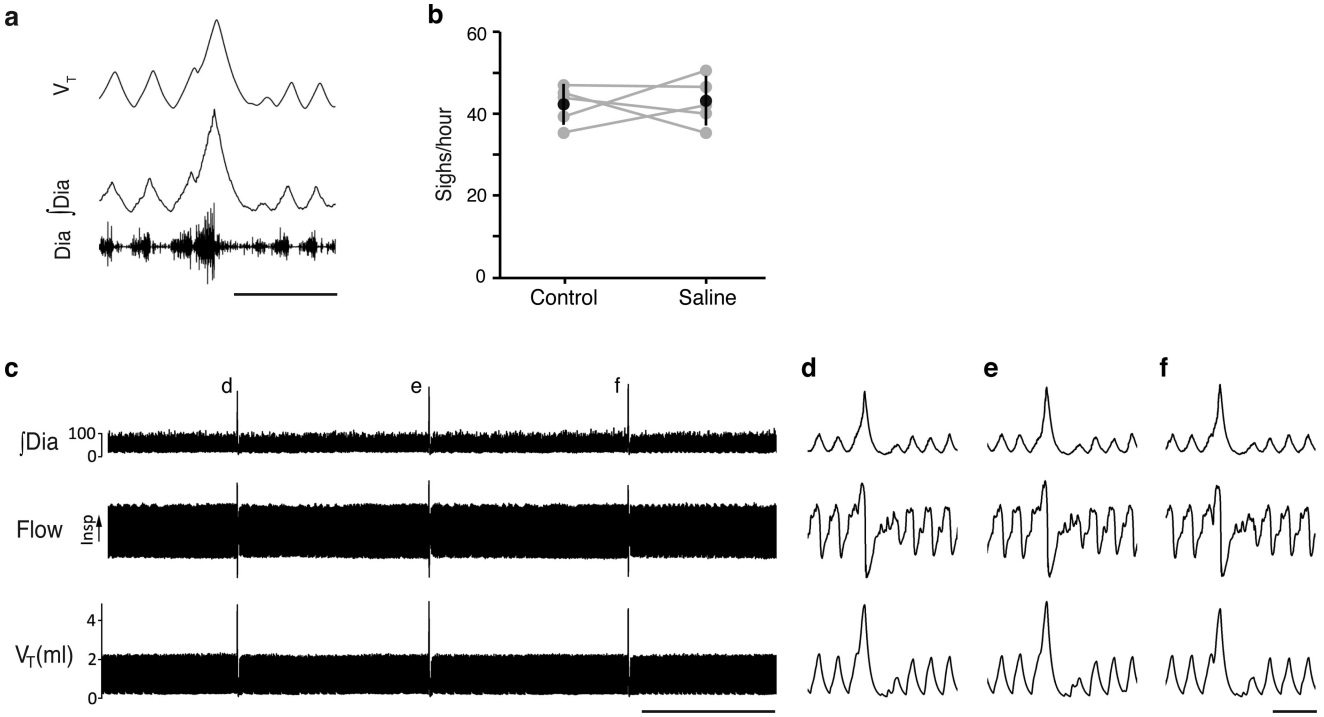

Extended Data Figure 3. Sighing after surgery and bilateral injection of saline into preBötC

a, Example of a sigh in a breathing activity trace of a urethane-anesthetized rat after surgery as in Fig. 2a-c. V_T, tidal volume; ∫Dia, integrated diaphragm activity; Dia, raw diaphragm activity trace. **b,** Sigh rate before (control) and after (saline) bilateral saline injection into preBötC. There is no effect of saline injection (n=5, p=0.83). **c-f,** Breathing activity trace as in a (but also showing airflow). Note stereotyped waveform of sighs (d-f). Bars, 1.min (c), 1 second (d-f).

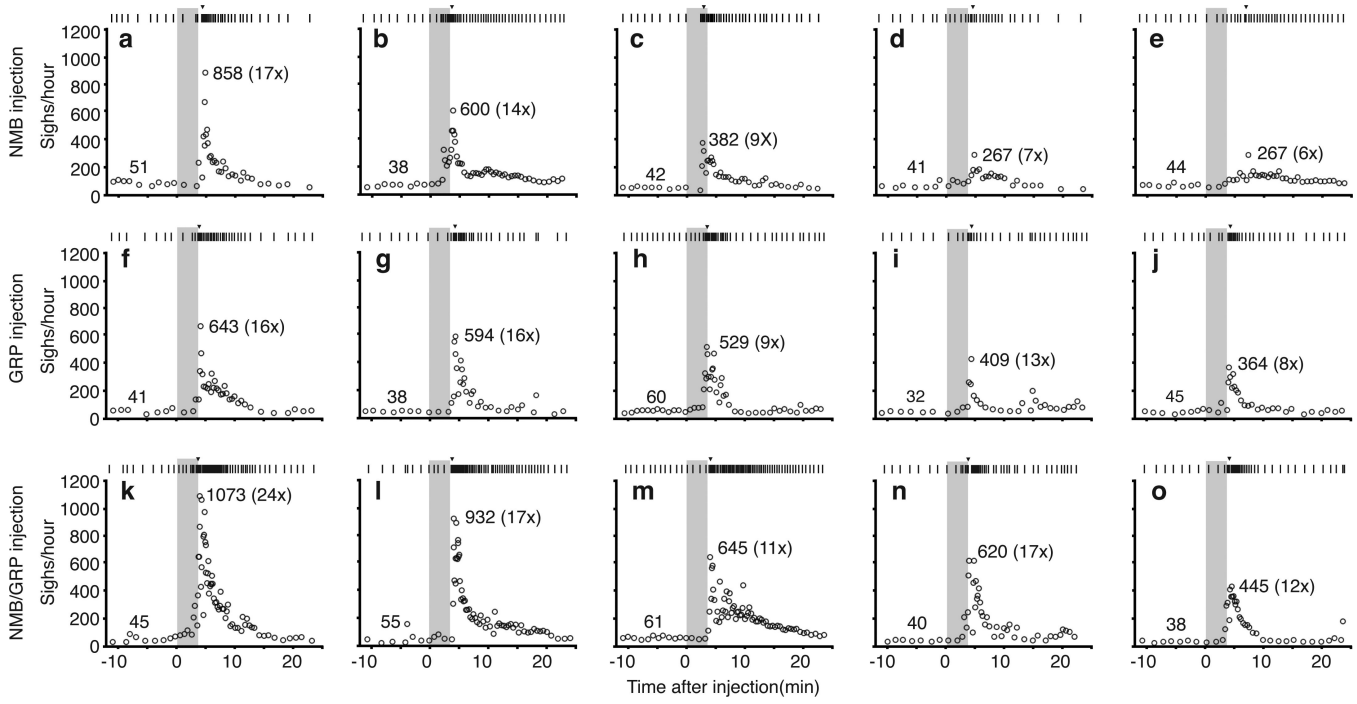

Extended Data Figure 4. Effects on sighing in individual rats following bilateral injection into preBötC of NMB, GRP and both NMB/GRP

a-e, Raster plot of sighs (upper) and instantaneous sigh rates (lower) before and after NMB injection for the five experiments (a-e) shown in Figure 2d. **f-j**, Raster plot of sighs (upper) and instantaneous sigh rates (lower) before and after GRP injection for the five experiments (f-j) shown in Figure 3c. **k-o**, Raster plot of sighs (upper) and instantaneous sigh rates (lower) before and after NMB/GRP injection for the five experiments (k-o) shown in Figure 4i. Grey, injection period; arrowhead in raster plots, maximum instantaneous sigh rate; numbers, basal (left) and maximal instantaneous sigh rate (right) and fold induction (in parentheses) after neuropeptide injection.

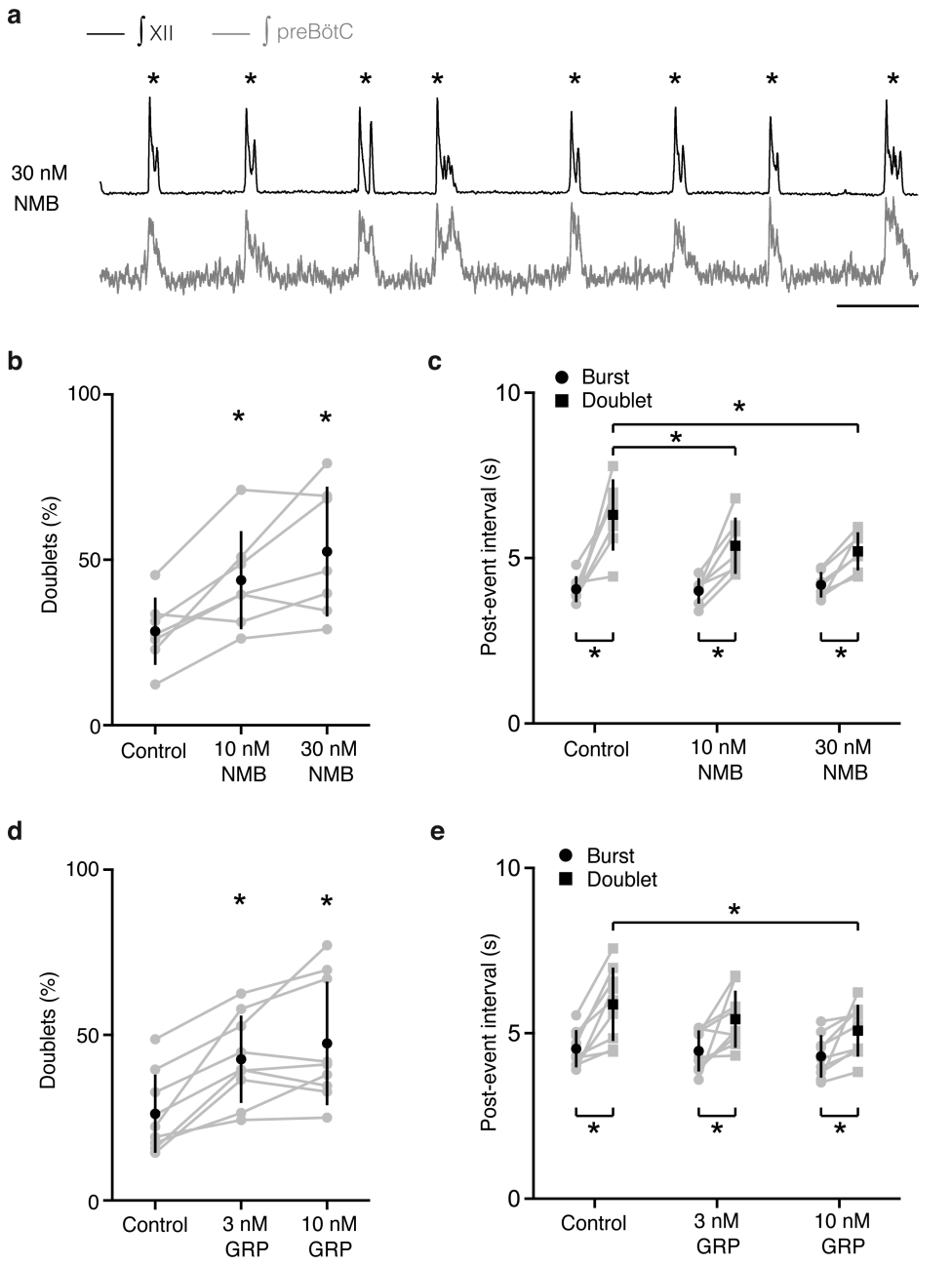

Extended Data Figure 5. Effect of NMB on rhythmic activity of preBötC slice

a, Neuronal activity trace (∫XII, black; ∫preBötC population activity, grey) of preBötC slice containing 30 nM NMB, as in Figure 2e. Note the extreme effect of NMB in which every burst ("breath") in the trace is a doublet ("sigh", *). Bar, 5 s. **b,c,** NMB increases the doublet rate by increasing the fraction of total events that are doublets (b) and decreasing the interval following a doublet (c). *, $p<0.05$, n=7. **d,e,** GRP also increases the doublet rate by increasing the fraction of total events that are doublets (d) and decreasing the interval following a doublet (e). *, $p<0.05$, n=9. Note that post-doublet intervals are significantly longer than post-burst intervals under all conditions, consistent with longer post-sigh apneas *in vivo*.

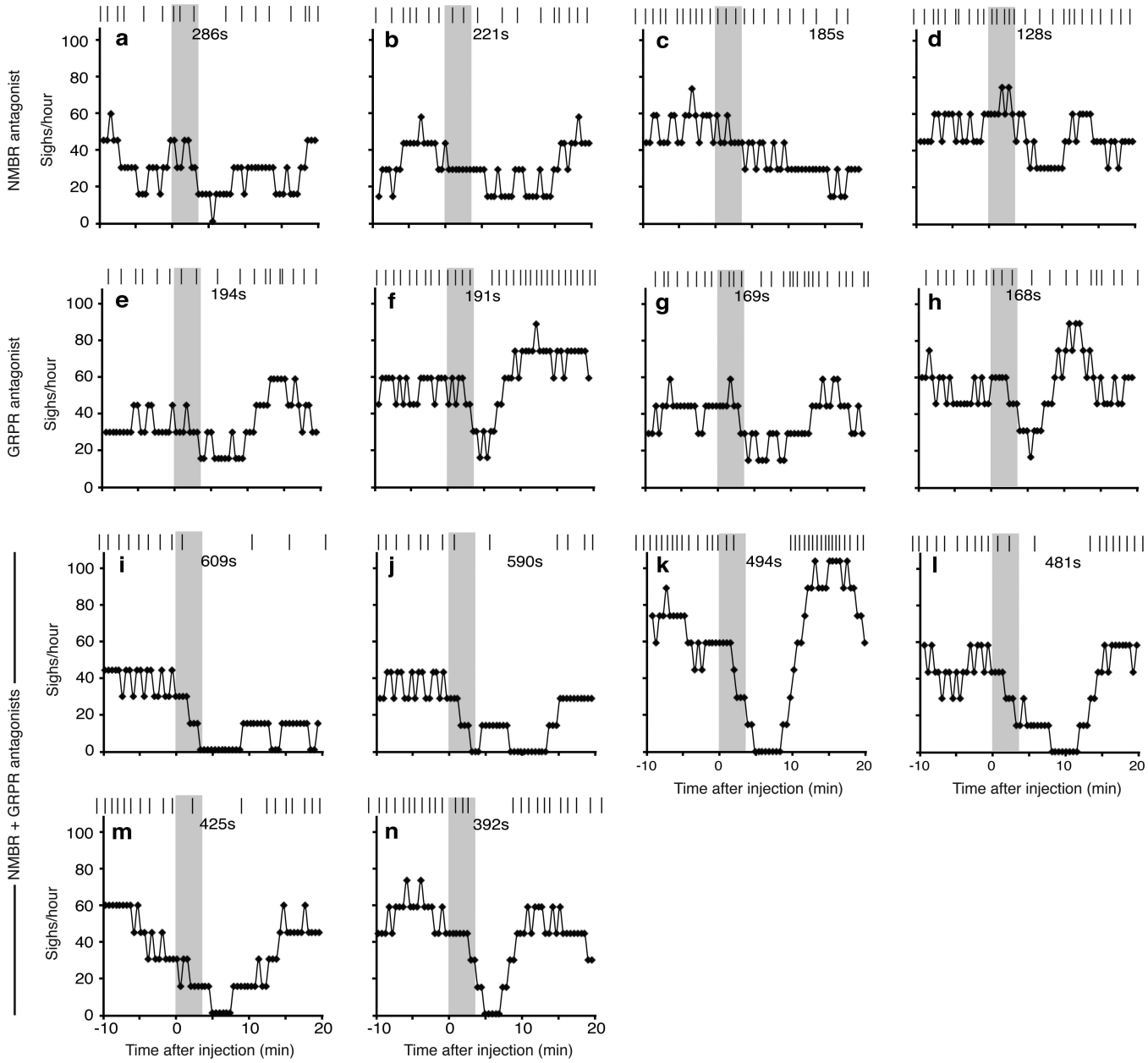

Extended Data Figure 6. Effects on sighing in individual rats following bilateral injection of BIM23042, RC3095 and BIM23042/RC3095 into preBötC

a-d, Raster plot of sighs (upper) and binned sigh rates (lower; bin size 4 min; slide 30s) before and after injection of the NMBR antagonist BIM23042 for the four experiments shown in Figure 2h. **e-h**, Raster plot of sighs (upper) and binned sigh rates (lower; bin size 4 min; slide 30s) before and after injection of the GRPR antagonist RC3095 for the four experiments shown in Figure 3f. **i-n**, Raster plot of sighs (upper) and binned sigh rates (lower; bin size 4 min; slide 30s) before and after BIM23042 and RC3095 injection for the six experiments shown in Figure 4j. Grey, injection period; numbers, longest intersigh intervals (s, seconds) following injection.

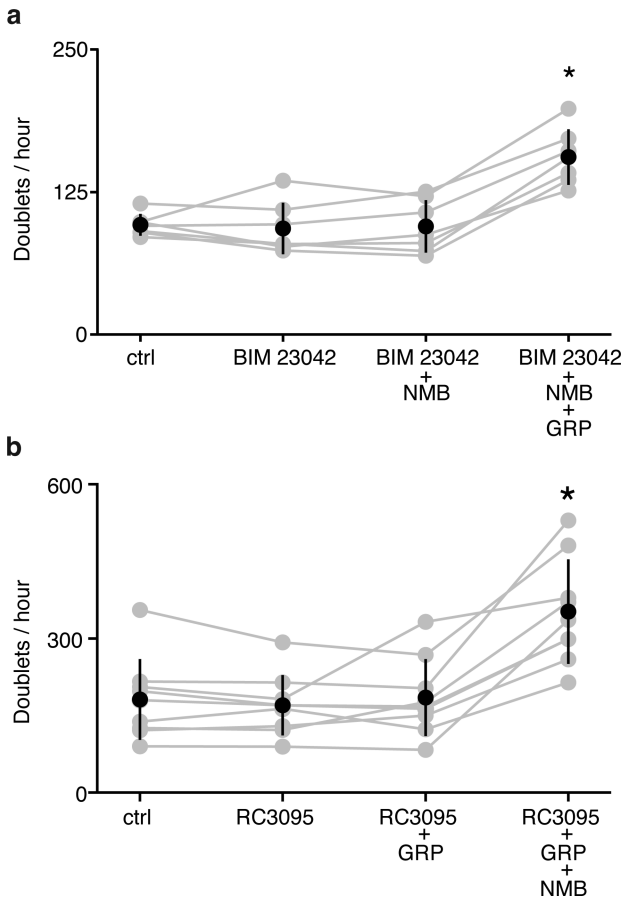

Extended Data Figure 7. Specificity of antagonists BIM23042 and RC3095 in preBötC slice

a, BIM 23042 (100 nM) blocks the effect of NMB (10 nM), but not GRP (3 nM) in preBötC slices. *, $p<0.05$, n=7. **b,** RC3095 (100 nM) shows the opposite specificity, blocking the effect of GRP (3 nM), but not NMB (10 nM) . *, $p<0.05$, n=9.

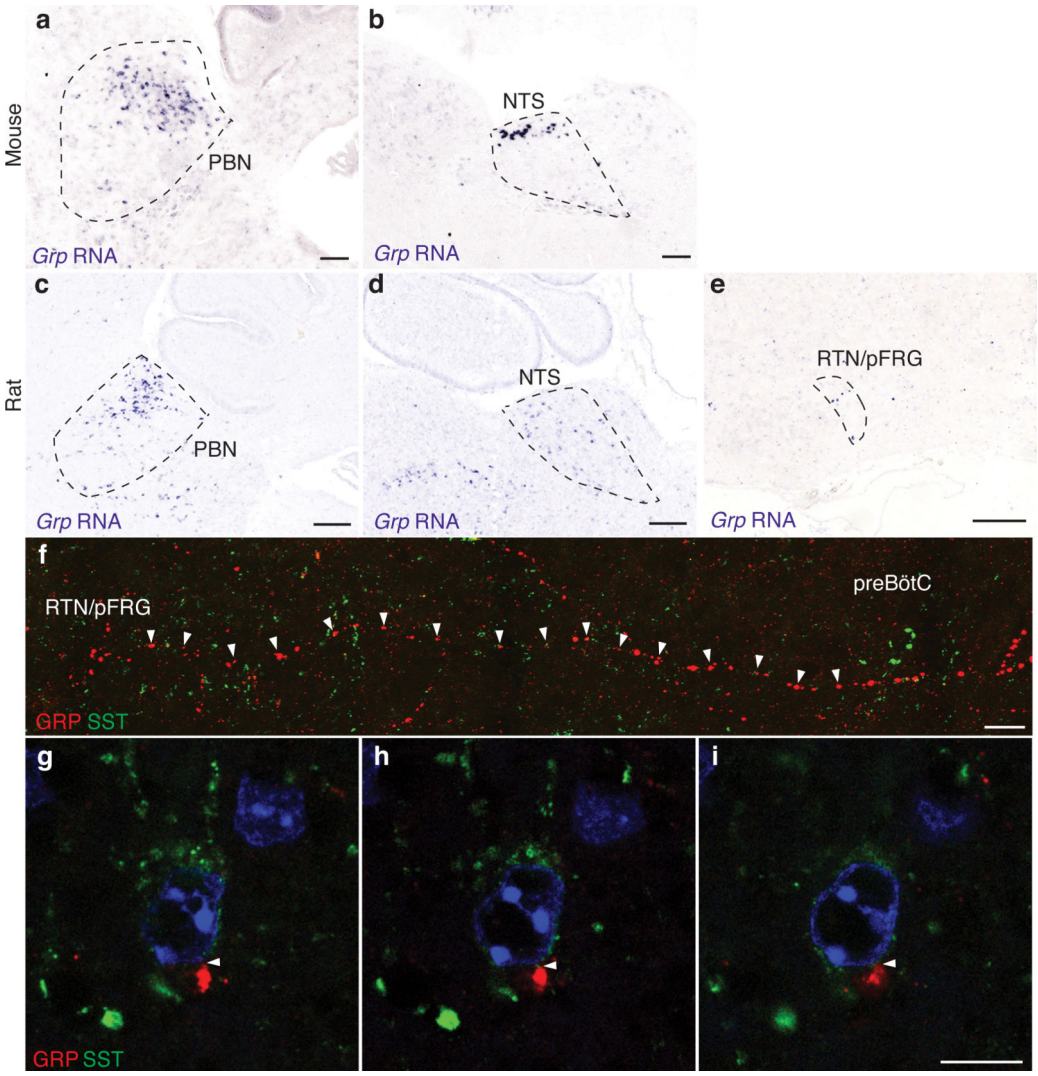

Extended Data Figure 8. Expression of *Grp* in rodent brain

a,b, *In situ* hybridization of mouse brain slices as in Figure 3a showing expression of *Grp* (purple) in parabrachial nucleus (PBN) (a) and nucleus tractus solitarius (NTS) (b). Bar, 200 μm. **c-e,** In situ hybridization of rat brain slices showing expression of *Grp* in PBN (c), NTS (d), RTN/pFRG (e). Bar, 200 μm. **f,** Tiled image showing GRP-positive projection (red) from RTN/pFRG region to preBötC region containing SST-positive neuron (green). Bar, 20 μm. **g-i,** Serial confocal optical sections (0.8 μm apart) through mouse preBötC stained for GRP (red) and SST (green) focusing on short segment of GRP-positive projection where a GRP puncta (red) directly abuts (arrowhead) an SST-positive neuron. Bar, 10 μm.

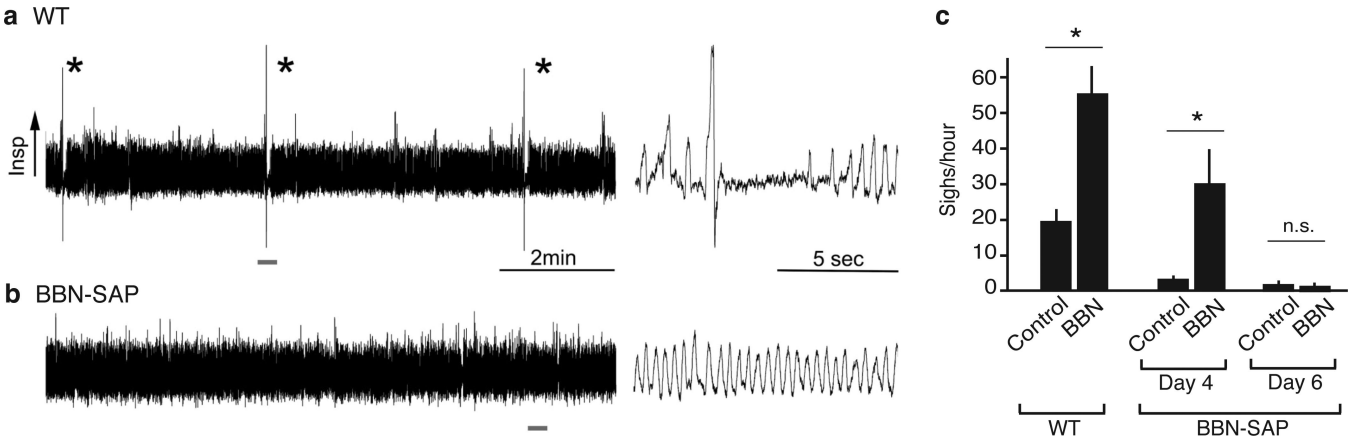

Extended Data Figure 9. Effect of bombesin injection on sighing following bombesin-saporin (BBN-SAP)-induced ablation of NMBR and GRPR-expressing preBötC neurons

a, b, 10 min plethysmography traces of a control rat (a) and a day 5 BBN-SAP injected rat (b) during eupneic breathing (left). Indicated parts (10 secs) of traces are expanded at right. Note presence of sighs with stereotyped waveform in control rat, and no sighs detectable in BBN-SAP injected rat. **c,** Sigh rate before (Control) and after 10 μg bombesin injection (BBN) into the preBötC of rats prior to BBN-SAP injection (WT) and at day 4 and day 6 after BBN-SAP injection (BBN-SAP) into the preBötC to ablate NMBR and GRPR-expressing neurons as in Figure 5a, b. Values shown are mean ± S.D. (WT, n=10; BBN-SAP, n=7 for day 4 and n=5 for day 6), *, $p<0.05$; n.s., not significant.

Supplementary Material

Refer to Web version on PubMed Central for supplementary material.

Acknowledgements

We thank M. Sunday for providing the *Nmbr*$^{-/-}$ and *Grpr*$^{-/-}$ mice, Y. Zhang for providing rat tissues, and K. Wada and E. Wada for plasmid constructs for *in situ* hybridization probes. We also thank members of the Krasnow and Feldman laboratories for helpful comments. This work was supported by the Howard Hughes Medical Institute (M.A.K.), NIH grants HL70029, HL40959 and NS72211 (J.L.F.), a Walter V. and Idun Berry postdoctoral fellowship (P.L.), the NIH Medical Scientist Training Program (K.Y.), and CIHR and AIHS postdoctoral fellowships (S.P.). M.A.K. is an investigator of the Howard Hughes Medical Institute.

References

1. Haldane JS, Meakins JC, Priestley JG. The effects of shallow breathing. Journal of Physiology. 1919; 52:433–453. [PubMed: 16993408]
2. McCutcheon FH. Atmospheric respiration and the complex cycles in mammalian breathing mechanisms. J. Cell. Physiol. 1953; 41:291–303. [PubMed: 13052646]
3. Knowlton GC, Larrabee MG. A unitary analysis of pulmonary volume receptors. Am. J. Physiol. 1946; 147:100–114. [PubMed: 21000728]
4. Reynolds LB. Characteristics of an inspiration-augmenting reflex in anesthetized cats. J Appl. Physiol. 1962; 17:683–688. [PubMed: 14491719]
5. Bartlett D. Origin and regulation of spontaneous deep breaths. Respir. Physiol. 1971; 12:230–238. [PubMed: 5568463]
6. Maytum CK. Sighing dyspnea: A clinical syndrome. Journal of Allergy. 1938; 10:50–55.

7. Smith JC, Ellenberger HH, Ballanyi K, Richter DW, Feldman JL. Pre-Bötzinger complex: a brainstem region that may generate respiratory rhythm in mammals. Science. 1991; 254:726–729. [PubMed: 1683005]
8. Gray PA, Janczewski WA, Mellen N, McCrimmon DR, Feldman JL. Normal breathing requires preBötzinger complex neurokinin-1 receptor-expressing neurons. Nat. Neurosci. 2001; 4:927–930. [PubMed: 11528424]
9. Tan W, et al. Silencing preBötzinger complex somatostatin-expressing neurons induces persistent apnea in awake rat. Nat. Neuroscience. 2008; 5:538–540. [PubMed: 18391943]
10. Feldman JL, Del Negro CA, Gray PA. Understanding the rhythm of breathing: so near, yet so far. Annu. Rev. Physiol. 2013; 75:423–452. [PubMed: 23121137]
11. Kam K, Worrell JW, Janczewski WA, Cui Y, Feldman JL. Distinct inspiratory rhythm and pattern generating mechanisms in the preBötzinger complex. J. Neurosci. 2013; 33:9235–9245. [PubMed: 23719793]
12. Lieske SP, Thoby-Brisson M, Telgkamp P, Ramirez JM. Reconfiguration of the neural network controlling multiple breathing patterns: eupnea, sighs and gasps. Nat. Neurosci. 2000; 3:600–607. [PubMed: 10816317]
13. Ruangkittisakul A, et al. Generation of eupnea and sighs by a spatiochemically organized inspiratory network. J. Neurosci. 2008; 28:2447–2458. [PubMed: 18322090]
14. Caughey JL Jr. Analysis of breathing patterns. Am. Rev. Tuberc. 1943; 48:382.
15. Niewoehner DE, Levine AS, Morley JE. Central effects of neuropeptides on ventilation in the rat. Peptides. 1983; 4:277–281. [PubMed: 6195647]
16. Ramirez JM. The integrative role of the sigh in psychology, physiology, pathology, and neurobiology. Prog. Brain Res. 2014; 209:91–129. [PubMed: 24746045]
17. Janczewski WA, Pagliardini S, Cui Y, Feldman JL. Sighing after vagotomy, Abstract No. 796.05 (Society of Neuroscience. New Orleans. 2012
18. Smith JC, Morrison DE, Ellenberger HH, Otto MR, Feldman JL. Brainstem projections to the major respiratory neuron populations in the medulla of the cat. J. Comp. Neurol. 1989; 281:69–96. [PubMed: 2466879]
19. Onimaru H, Homma I. A novel functional neuron group for respiratory rhythm generation in the ventral medulla. J. Neurosci. 2003; 23:1478–1486. [PubMed: 12598636]
20. Diez-Roux G, et al. A high resolution atlas of the transcriptome in the mouse embryo. Plos Biology. 2011; 9:e1000582. [PubMed: 21267068]
21. Mulkey DK, et al. Respiratory control by ventral surface chemoreceptor neurons in rats. Nat. Neurosci. 2004; 7:1360–1369. [PubMed: 15558061]
22. Stornetta RL, et al. Expression of Phox2b by brainstem neurons involved in chemosensory integration in the adult rat. J. Neurosci. 2006; 26:10305–10314. [PubMed: 17021186]
23. Guyenet PG, Bayliss DA. Neural control of breathing and CO2 homeostasis. Neuron. 2015; 87:946–961. [PubMed: 26335642]
24. Lazarenko RM, et al. Acid sensitivity and ultrastructure of the retrotrapezoid nucleus in Phox2b-EGFP transgenic mice. J. Comp. Neurol. 2009; 517:69–86. [PubMed: 19711410]
25. Bendixen HH, Smith GM, Mead J. Pattern of ventilation in young adults. J. of Appl. Phys. 1964; 19:195–198.
26. Jensen RT, et al. International Union of Pharmacology. LXVIII. Mammalian bombesin receptors: nomenclature, distribution, pharmacology, signaling, and functions in normal and disease states. Pharmacol Rev. 2008; 60:1–42. [PubMed: 18055507]
27. Guyenet PG, Stornetta RL, Bayliss DA. Central respiratory chemoreception. J. Comp. Neurol. 2010; 518:3883–3906. [PubMed: 20737591]
28. Lee H, Naughton NN, Woods JH, Ko MC. Characterization of scratching responses in rats following centrally administered morphine or bombesin. Behav. Pharmacol. 2003; 14:501–508. [PubMed: 14557717]
29. Pagliardini S, et al. Active expiration induced by excitation of ventral medulla in adult anesthetized rats. J. Neurosci. 2011; 31:2895–905. [PubMed: 21414911]

30. Ohki-Hamazaki H, et al. Functional properties of two bombesin-like peptide receptors revealed by the analysis of mice lacking neuromedin B receptor. J. Neurosci. 1999; 19:948–954. [PubMed: 9920658]

31. Wada E, et al. Generation and characterization of mice lacking gastrin-releasing peptide receptor. Biochem Biophys Res Commun. 1997; 239:28–33. [PubMed: 9345264]

32. Tomer R, et al. Advanced CLARITY for rapid and high-resolution imaging of intact tissues. Nature Protoc. 2014; 9:1682–1697. [PubMed: 24945384]

33. Obruch M, et al. Discovery of a novel class of neuromedin B receptor antagonists, substituted somatostatin analogues. Mol Pharmacol. 1993; 44:841–850. [PubMed: 7901752]

34. Qin Y, et al. Inhibitory effect of bombesin receptor antagonist RC-3095 on the growth of human pancreatic cancer cells in vivo and in vitro. Cancer Res. 1994; 54:1035–1041. [PubMed: 8313359]

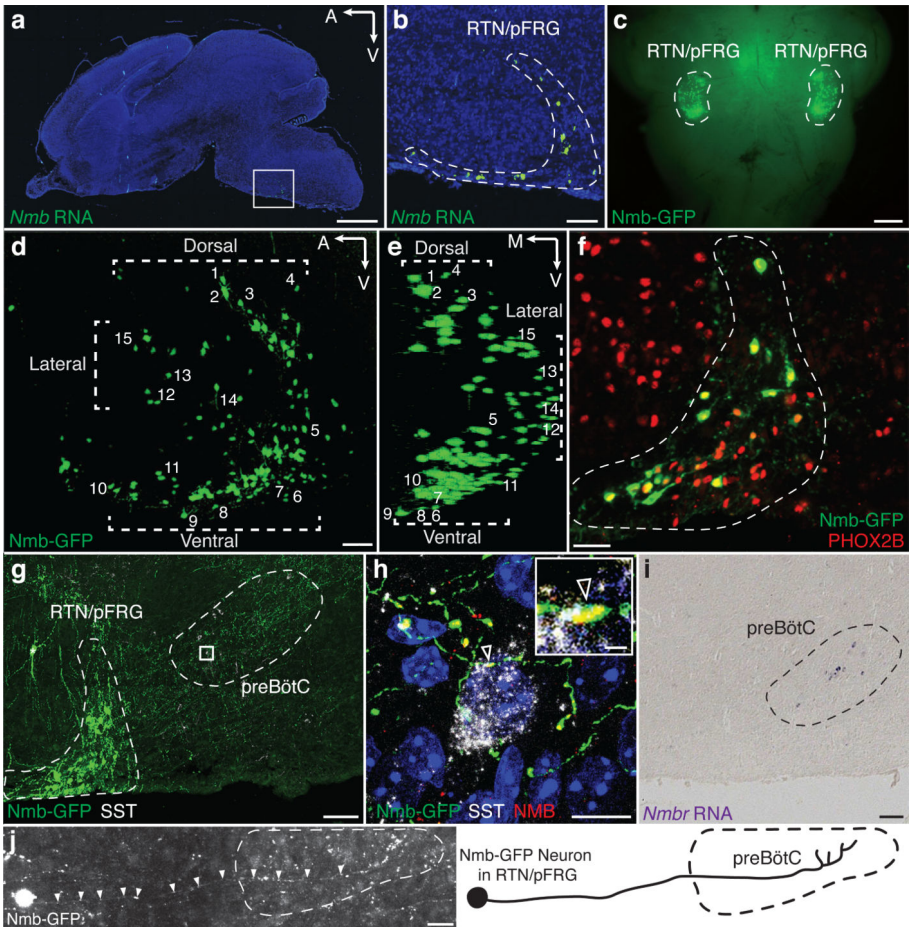

Figure 1. NMB neuropeptide pathway neurons in breathing center

a, P0 mouse brain section probed for *Nmb* mRNA (green) with DAPI counterstain (nuclei, blue). Bar, 1mm. **b,** Boxed region (a) showing specific expression in RTN/pFRG. Bar, 100μm. **c,** Whole mount P0 brainstem (ventral view) showing Nmb-GFP transgene expression (GFP, green) bilaterally in RTN/pFRG. Bar, 0.5mm. **d,e**, 3D reconstruction (sagittal (d), coronal (e) projections) of CLARITY-cleared P14 Nmb-GFP brainstem. Note RTN/pFRG expression ventral, dorsal, and lateral to facial nucleus. Numbers, representative neurons. A,anterior; V,ventral; M,medial. Bar, 100μm. **f,** P0 Nmb-GFP-expressing neurons (green) in RTN/pFRG (dashed) co-express RTN marker PHOX2B (red). Bar, 50μm. **g,** P7 Nmb-GFP-expressing neurons (green) project to preBötC (dashed). SST (somatostatin), preBötC marker (white). *, isolated GFP-labeled neuron in facial nucleus. Bar, 100μm. **h,** Boxed region (**g)** with NMB co-stain (z-stack projection; optical sections, ED Fig. 2). Arrowhead, NMB puncta (red) in Nmb-GFP-expressing projection (green) abutting preBötC neuron (SST, white). Bars, 10μm (1μm, inset). **i,** P7 ventral medulla section probed for *Nmbr* mRNA (purple) showing preBötC expression. Bar, 100μm. **j,** Tiled image (left) and tracing (right) of Nmb-GFP neuron as in (**g**) projecting to preBötC. Bar, 30μm.

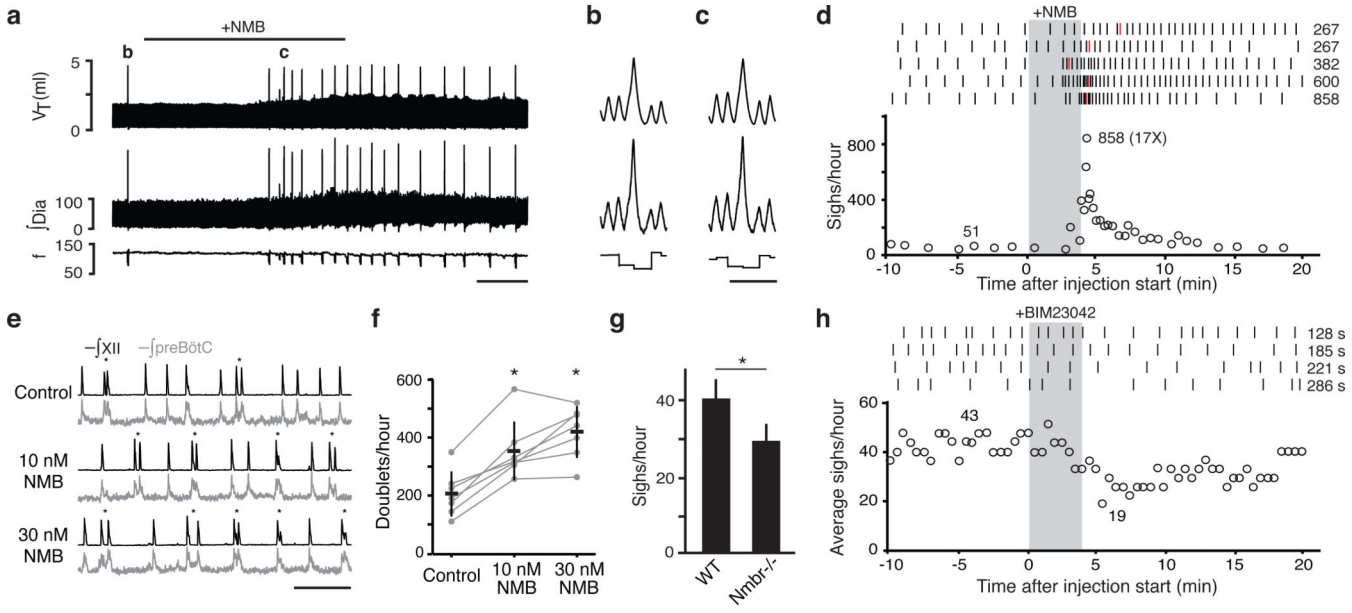

Figure 2. NMB effect on breathing

a-c, Breathing activity of anesthetized rat following bilateral NMB injection (100nl, 3μM) into preBötC. Note increased sighing (spikes in tidal volume (V_T), integrated diaphragm activity (∫Dia)) but little change in respiratory rate (frequency, f). Bar, 1 min. **b,c,** Similar, stereotyped waveforms of spontaneous (b) and NMB-induced (c) sighs (from a; also ED Fig. 3a,c-f). Bar, 2s. **d**, Quantification of (a). Top: raster plots of sighs (tics) in five rats following NMB injection (grey); numbers, highest instantaneous sigh rate (red tics). Bottom: instantaneous sigh rate of bottom raster plot; numbers, average instantaneous sigh rate before and maximum (and fold increase) after injection. **e,** Integrated hypoglossal nerve (∫XII; black) and preBötC neural activity (∫preBötC; grey) in preBötC slices containing indicated NMB concentrations. NMB increases doublets (*), a sigh signature in slices. Bar, 10s. **f,** Quantification of (e) (n=7; *, $p<0.05$). **g**, Basal sigh rate in C57BL/6 wild-type (WT) and *Nmbr*$^{-/-}$ mice. n=4; bars, standard deviation of mean; *, $p<0.001$. **h**, Effect on sighing in anesthetized rats of bilateral preBötC injection (grey) of NMBR antagonist BIM23042 (100nl, 6μM). Top: raster plots; numbers, longest intersigh intervals (s, seconds) following injection. Bottom: sliding average sigh rate (bin 4 min; slide 30s); numbers, average rate before (left) and minimum binned rate after injection (right).

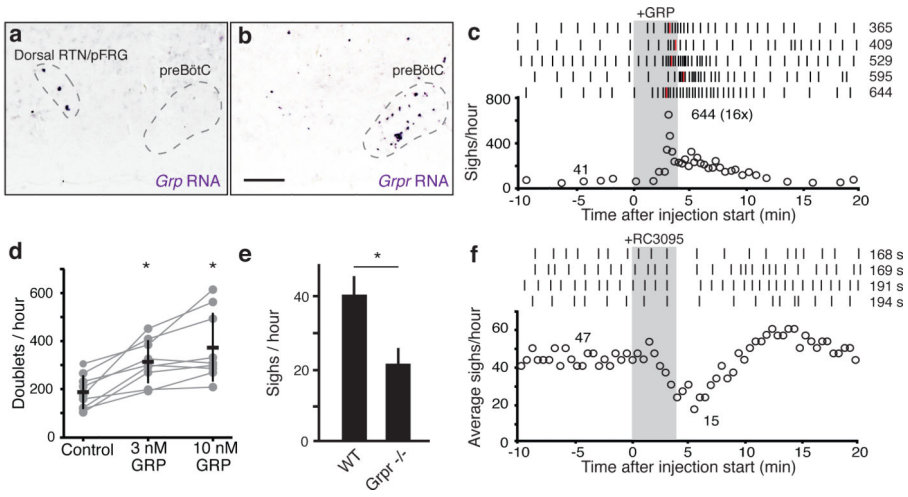

Figure 3. GRP neuropeptide pathway expression and function in breathing

a-b, Sagittal ventral medulla sections of P7 mice probed for *Grp* (a) or *Grpr* (b) mRNA (purple). Bar, 200μm. **c**, Effect on sighing of bilateral preBötC injection of GRP (100nl, 3μM), as in Fig. 2d. **d**, Effect of GRP on doublets (sighs) in preBötC slices, as in Fig. 2f. n=9; *, $p<0.05$. **e**, Basal sigh rate in C57BL/6 wild-type (WT) and $Grpr^{-/-}$ mice, as in Fig. 2g. **f**, Effect on sighing of bilateral preBötC injection of GRPR antagonist RC3095 (100nl, 6μM), as in Fig. 2h.

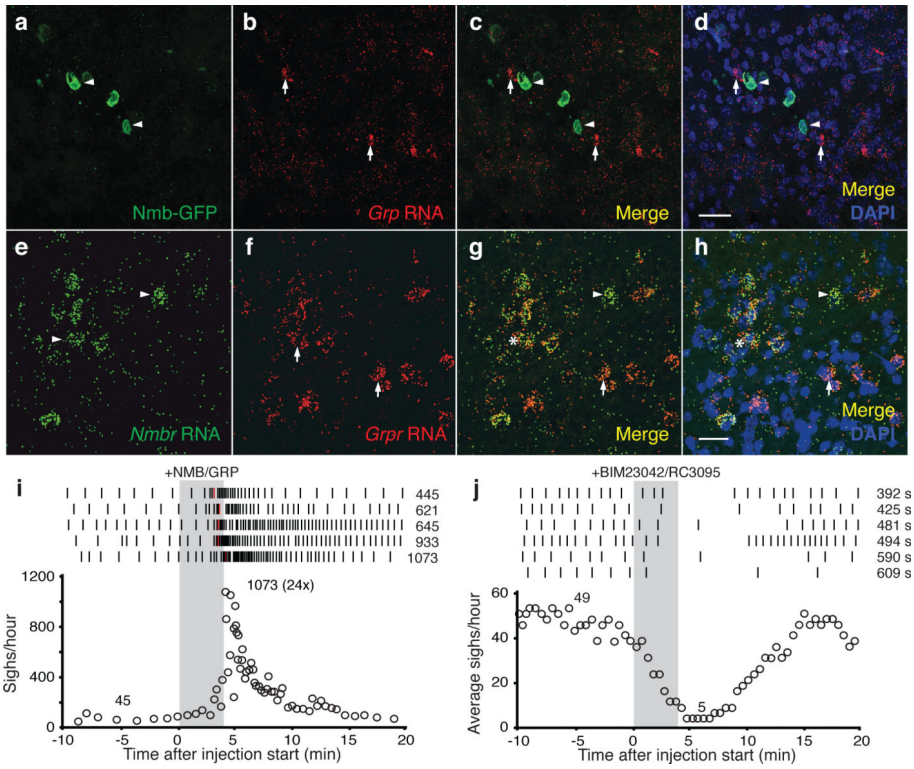

Figure 4. Interactions between NMB and GRP pathways in sighing

a-d, RTN/pFRG section of P7 Nmb-GFP mouse immunostained for GFP (green, arrowheads) and probed for *Grp* mRNA (red, arrows). Note no expression overlap. Bar, 30μm. **e-h**, preBötC section of P28 mouse probed for *Nmbr* mRNA (green, arrowheads) and *Grpr* mRNA (red, arrows). Note partial expression overlap. Bar, 30μm. **i**, Effect on sighing of bilateral preBötC injection of both NMB (100nl, 3μM) and GRP (100nl, 3μM) as in Fig. 2d. **j**, Effect on sighing of bilateral preBötC injection (100nl, 6μM) of both NMBR and GRPR antagonists (BIM23042, RC3095) as in Fig. 2h.

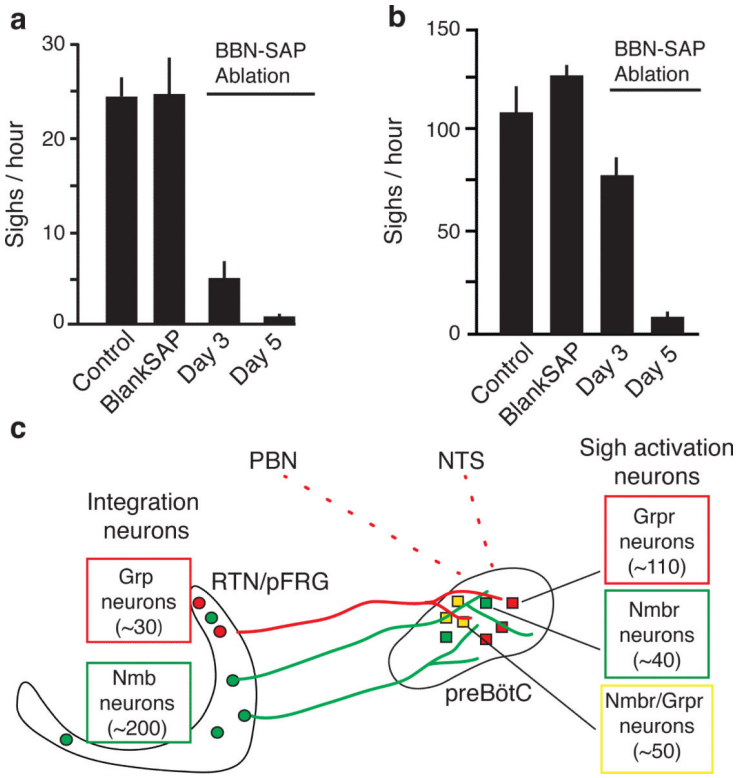

Figure 5. Effect on sighing of ablating preBötC NMBR-expressing and GRPR-expressing neurons

a,b, Basal (**a**) and hypoxia-induced (**b**) sigh rates before (control) and 3 or 5 days after preBötC injections of bombesin-saporin (200nl, 6.2ng; BBN-SAP ablation) to ablate NMBR and GRPR expressing neurons, or 5 days after saporin alone (200nl, 6.2ng; Blank-SAP). **c**, Model of peptidergic sigh control circuit. NMB- and GRP-expressing neurons in RTN/pFRG (and perhaps GRP-expressing neurons in NTS and PBN) receive physiological and perhaps emotional input from other brain regions, stimulating neuropeptide secretion. This activates receptor-expressing preBötC neurons expressing their receptors, which transform the normal preBötC rhythm to sighs. (Because neuropeptides induce sighs separated by normal breaths (Figure 2A), there must be some refractory mechanism in or downstream of receptor-expressing neurons that temporarily prevents a second sigh.)